

# ASYMMETRIC GAUSSIAN CHIRPLET MODEL FOR ULTRASONIC ECHO ANALYSIS

Ramazan Demirli

Center for Advanced Communications  
Villanova University, Villanova, PA 19085 USA  
e-mail: ramazan.demirli@villanova.edu

Jafar Saniie

Department of Electrical & Computer Engineering  
Illinois Institute of Technology  
Chicago, IL, 60616 USA

**Abstract-** Parametric modeling and estimation of ultrasonic backscattered echoes become a frequently used approach in NDE signal processing. Compared to classical transform based signal processing methods, the parametric echo representation approach offers significant advantages such as high-resolution estimation of test parameters (e.g., time-of-arrival, center frequency, and amplitude), the ability to resolve closely spaced overlapping echoes, and robustness with noise. In this context, parametric models such as Gaussian echo (Gabor function) and Gaussian Chirplet have been used to represent discrete echoes. Furthermore, their composite models have been used to analyze complex ultrasonic measurements such as overlapping echoes from thin layers, backscattered echoes from microstructure of materials, etc. One of the main shortcomings of these models is that their symmetric envelope does not properly represent ultrasonic echo envelopes. A more generic model accounting for this asymmetry will improve ultrasonic echo parameter estimation, (e.g., time-of-arrival, center frequency, bandwidth, chirp rate, etc.), as well as improve sparse decomposition of complex ultrasonic signals. In this study, we introduce the asymmetric Gaussian Chirplet (AGC) model that generalizes the existing parametric echo models. We developed a fast supervised Gauss-Newton algorithm to estimate model parameters subject to constraints defined by a priori knowledge. Supervision ensures convergence to the optimal solution given a reasonable initial guess. This echo model nicely fits echoes acquired from planar surface and geometric reflectors. Finally, this model is used to estimate microstructure grain echoes from a steel block and reverberation echoes from a multi-layered material. Estimation results confirm the advantage of this model compared to the existing models.

## I. INTRODUCTION

Parametric modeling and estimation of ultrasonic backscattered echoes have been introduced in [1, 2] and become a frequently used approach in NDE signal processing. Compared to classical transform based ultrasonic signal processing methods, the parametric echo representation approach offers significant advantages such as high-resolution estimation of test parameters (e.g., time-of-arrival, center frequency, and amplitude), the ability to resolve closely spaced overlapping echoes, and robustness with noise. Parametric modeling concept has been widely accepted in ultrasonic NDE studies, for example, ultrasonic data compression [3], Chirplet signal decomposition [4], sizing of cracks in thin sections [5], the assessment of the bone structural parameters [6], and structural health monitoring of materials [7]. Most of these studies utilized the Gaussian echo model (i.e., real Gabor function) to represent backscattered echoes. Gaussian echo model is essentially a Gaussian modulated sinusoid with five parameters (time-of-arrival, center frequency, bandwidth, phase, and amplitude) and provides a good approximation to a backscattered echo from a point or surface reflector. This approximation is not always adequate especially for cases in

which accurate estimation of the pulse shape is critical as in ultrasonic deconvolution [2]. For example, in thickness sizing of thin layers, the received echoes are often overlapping and resolution of these echoes relies on accurate estimation of the pulse-echo wavelet. To represent complex shape echoes, the composite Gaussian echoes model has been introduced [2]. The composite echoes model involves estimating the transducer pulse in terms of a number of overlapping Gaussian echoes. Therefore, the composite model parameters do not have a direct interpretation for echo signal parameters.

Despite the shortcomings of Gaussian echo model in representing discrete echoes, it has been extensively used in sparse signal decomposition algorithms [3, 4, 8]. In fact, long before it is used as a parametric model in ultrasonic signal processing it had been used as an elementary signal to generate Gabor dictionary functions in Mallat's generic sparse signal decomposition method, i.e., the well-known Matching Pursuit (MP) algorithm [9]. The Gabor dictionary has been frequently used for ultrasonic signal decomposition because Gabor functions highly correlate with ultrasound echoes. Later, the model-based MP method [8] is introduced to allow more flexibility in sparse decomposition by optimizing the parameters of the Gaussian echo model to match ultrasound echo structures. In short, this model has proved to be useful in sparse decomposition of ultrasonic echoes. However, the decomposed echo components do not necessarily represent the real echo structures.

Later, in sparse signal decomposition studies, Gaussian echo model has been generalized to the Gaussian Chirplet with the addition of an extra chirp parameter in the sinusoid to allow a linear drift in frequency. This type of model has been used in [4] and in [10] for a generic decomposition of an acoustic signal in terms of Gaussian Chirplets. Although this model is better than the Gaussian echo model in representing dispersive echoes, the envelope of this model is still a Gaussian shape and symmetric with respect to its peak location. The Gaussian envelope models are insufficient to represent echoes with a non-symmetric shape.

In this study we introduce a new parametric echo model that has an asymmetric and smooth envelope. This echo model is inspired from the electro-acoustic properties of the piezoelectric ultrasonic transducer. The envelope of the echo rapidly rises until the peak and slowly decays afterwards. To represent such an envelope, a smooth approximation of the asymmetric Gaussian function is utilized. This model is a generalization of the existing Gaussian echo and Gaussian chirplet models.

The rest of the paper is organized as follows. The next section introduces the new Asymmetric Gaussian Chirplet (AGC) model and echo parameters related to NDE testing. Section III presents an optimization algorithm to estimate the

parameters of this model in the presence of measurement noise. This section also presents parameter estimation of echoes obtained from several different transducers and measurement conditions. Section IV discusses the application of this model to a sparse signal decomposition algorithm to represent complex ultrasonic measurements such as microstructure grain echoes from a steel block and reverberation echoes from a multi-layered material.

## II. ASYMMETRIC GAUSSIAN CHIRPLET MODEL

We represent a discrete ultrasonic echo (e.g., a backscattering echo from a planar surface reflector, or a point reflector) in terms of an envelope and a chirp sinusoidal component:

$$s(t) = \beta env(t - \tau) \cos \{2\pi f_c(t - \tau) + \psi(t - \tau)^2 + \phi\} \quad (1)$$

where  $\beta$  is the amplitude,  $\tau$  is the arrival time,  $f_c$  is the center frequency,  $\psi$  is the linear chirp rate, and  $\phi$  is the phase of the model echo. The envelope of the echo  $env(t)$  is represented by the following asymmetric Gaussian function:

$$env(t) = \exp(-\alpha(1 - r \tanh(mt))t^2) \quad (2)$$

where  $\alpha$  is the decay rate (bandwidth factor), and  $r$  is a coefficient controlling the degree of envelope asymmetry, and  $\tanh(mt)$  is *hyperbolic tangent* function of order  $m$  where  $m$  is a positive integer, e.g., 16. This function is a smooth approximation to a *sign* function and responsible for changing the sign of the parameter  $r$  in a very short period of time, in  $[-\varepsilon \ \varepsilon]$ . Therefore, the envelope function approximates to Gaussian functions with two different decay rates before and after the peak point, i.e.,

$$env(t) = \exp(-\alpha(1 - r)t^2), \quad t > \varepsilon \quad (3)$$

$$env(t) = \exp(-\alpha(1 + r)t^2), \quad t < -\varepsilon$$

for a very small positive number  $\varepsilon$ . For the above function to be a valid echo envelope (i.e., finite duration) the following conditions should hold:

$$i) \ \alpha > 0, \quad ii) \ -1 < r < 1$$

Before and after the reference point  $\tau$ , the envelope can have effectively two different decay rates  $\alpha_L$  and  $\alpha_R$ ,

$$\alpha_L = \alpha(1 + r), \quad \alpha_R = \alpha(1 - r) \quad (4)$$

The alternation of parameter  $\alpha$  alpha between  $\alpha_L$  and  $\alpha_R$  illustrated in Figure 1.b for a typical parameter set. The parameter  $r$  can be expressed in terms of the left and right half decay rates using Equation 4:

$$r = \frac{\alpha_L - \alpha_R}{\alpha_L + \alpha_R} \quad (5)$$

In summary, the parameters of the model are:

$\alpha_L$  : Decay rate for the left-half of envelope

$\alpha_R$  : Decay rate for the right-half of envelope

$\tau$  : Arrival time

$f_c$  : Center frequency

$\psi$  : Chirp rate

$\phi$  : Phase

$\beta$  : Amplitude

For  $\alpha_L = \alpha_R$  ( $r = 0$ ) the envelope in Equation 2 reduces to a Gaussian function and the model in Equation 1 simplifies to the Gaussian Chirplet model. Furthermore, when the Chirp rate is zero, the model reduces to the Gaussian Echo model. Therefore, this model generalizes these two existing echo models. For typical values of parameters,  $\theta = [\alpha \ r \ \tau \ f_c \ \psi \ \phi \ \beta] = [10 \ 0.5 \ 1\mu s \ 5MHz \ -1 \ 0 \ 1]$  the realization of the model echo is shown in Figure 1.a, the change of parameter  $\alpha$  during echo period is shown in Figure 1.b, and its magnitude spectrum is shown in Figure 1.c.

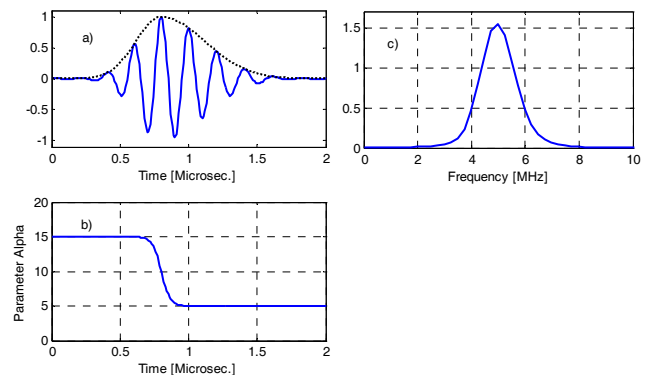


Figure 1. An example of an asymmetric Gaussian Chirplet echo with typical parameters, a) Time-domain representation (solid line) and its envelope (dotted line), b) The change of parameter alpha with time, c) Magnitude spectrum.

The AGC has desirable mathematical properties (n-th order integrable and differentiable) and is convenient for numerical calculations. This model allows the envelope to be asymmetric and ensures a monotonic rise and decay before and after the time-of-arrival. Most often, the symmetric envelope model is insufficient to represent echo envelopes that are often sharply rising before the peak and slowly decaying after.

Before we address parameter estimation, we note that echo signal characteristics and transforms (bandwidth, energy, Fourier transform, time-frequency representation) can be analytically derived in terms of model parameters. The energy of the AGC echo can be calculated as the energy of the envelope term since the energy of the sinusoidal is unity. The echo energy depends on the amplitude and decay rates ( $\alpha_L, \alpha_R$ ). The bandwidth of the echo depends on the decay rates ( $\alpha_L, \alpha_R$ ). Reference [1] outlines a procedure to derive the magnitude spectrum, energy and bandwidth of the echo.

## III. MAXIMUM LIKELIHOOD ESTIMATION OF AGC PARAMETERS

We now describe a procedure to estimate the parameters of the AGC model presented in Equation 1. An observed echo with measurement noise can be written as

$$y(t) = s(\theta; t) + v(t) \quad (6)$$

where  $s(\theta; t)$  is the AGC model (Equation 1) whose discrete version can be written as:

$$\begin{aligned} s(\theta; t_k) &= \text{env}(t_k - \tau) \cos\{2\pi f_c(t_k - \tau) + \psi(t_k - \tau)^2 + \phi\} \\ \text{env}(t_k - \tau) &= \exp(-\alpha(1 - r \tanh(m(t_k - \tau)))(t_k - \tau)^2) \quad (7) \\ k &= 0, 1, 2, \dots, K-1 \quad \text{and} \quad t \in [0 T_s] \end{aligned}$$

where  $t_k = kT$  is the discrete time samples and  $T$  is the sampling interval. The parameters of the model, bandwidth factor, asymmetry factor, arrival time, center frequency, chirp rate, phase and amplitude are stored in a parameter vector in this order as  $\theta = [\alpha \ r \ \tau \ f_c \ \psi \ \phi \ \beta]$ . The measurement noise  $v(t_k)$  can be modeled as white Gaussian noise (WGN), thus the Maximum Likelihood Estimator (MLE) of the parameter vector can be obtained by solving:

$$\hat{\theta} = \arg_{\theta} \min \|y - s(\theta)\|^2 \quad (8)$$

where  $y$  represents the measured echo sampled with a sampling frequency above the Nyquist rate. This non-linear LS problem can be solved with iterative least square optimization algorithms provided that the initial guess for the parameter vector is fairly close to the optimal solution. For example, reference [1] provides a fast Gauss-Newton (GN) algorithm for parameter estimation of the Gaussian echo model. This algorithm has been adapted for the AGC model, however it has been observed that the parameter estimation was heavily dependent on the initial guess. In particular, the estimation of the asymmetry factor proved to be challenging since this parameter should only change in the range (-1, 1). As a result we developed a supervised Gauss Newton (SGN) algorithm by utilizing the *Maximum a Posteriori Estimation* (MAP) principle. This principle provides a mechanism to control parameter estimation within specified bounds. This algorithm is formally presented next.

### Supervised Gauss Newton Algorithm

1. Set the initial guess and prior covariance matrix

$$\begin{aligned} \theta^{(n)} \text{ and } C_{\theta\theta} &= E[(\theta - \bar{\theta})(\theta - \bar{\theta})^T] \quad \text{and} \\ n &= 0 \quad (\text{outer loop iteration number}) \end{aligned}$$

2. Set the prior mean  $\mu_{\theta} = E[\theta] = \theta^{(n)}$  as the initial guess and set  $k = 0$  (inner loop iteration number).

3. Compute gradients  $H(\theta^{(k)})$  and the AGC model  $s(\theta^{(k)})$

4. Iterate the parameter vector via MAP estimation:

$$\begin{aligned} \tilde{x}^{(k)} &= y - s(\theta^{(k)}) + H(\theta^{(k)})\theta^{(k)} \\ \theta^{(k+1)} &= \mu_{\theta} + [C_{\theta\theta}^{-1} + \frac{1}{\sigma_w^2} H^T(\theta^{(k)})H(\theta^{(k)})]^{-1} H^T(\theta^{(k)}) \frac{1}{\sigma_w^2} [\tilde{x}^{(k)} - H(\theta^{(k)})\mu_{\theta}] \end{aligned}$$

5. Check inner-loop stop criteria:

$$\text{If } \|\theta^{(k+1)} - \theta^{(k)}\| < \textit{tolerance1} \text{ or } k > kMax,$$

Set  $\theta^{(n+1)} \rightarrow \theta^{(k+1)}$  and continue on Step 6.

Otherwise, set  $\theta^{(k)} \rightarrow \theta^{(k+1)}$ ,  $k \rightarrow k+1$  and go to Step 3.

6. Check global convergence:

$$\text{If } \|\theta^{(n+1)} - \theta^{(n)}\| < \textit{tolerance2}, \text{ STOP.}$$

Otherwise, set  $\theta^{(n)} \rightarrow \theta^{(n+1)}$ ,  $n \rightarrow n+1$  and go to Step 2.

Step 1 receives an initial guess and the predetermined covariance matrix for the parameter vector to control the variance from the prior means. Step 2 sets the prior mean as the initial guess for the parameter vector. Step 3 computes the gradients and the model in terms of new parameters. Step 4 implements the MAP estimation under the assumed Bayesian linear model [11],  $\tilde{x} = H(\theta)\theta + w$ , where  $w$  denotes a WGN vector with variance  $\sigma_w^2$ .  $H(\theta)$  in Step 4 denotes the gradient

$$\text{matrix, i.e., } H(\theta) = \begin{bmatrix} \frac{\partial s}{\partial \alpha} & \frac{\partial s}{\partial r} & \frac{\partial s}{\partial \tau} & \frac{\partial s}{\partial f_c} & \frac{\partial s}{\partial \psi} & \frac{\partial s}{\partial \phi} & \frac{\partial s}{\partial \beta} \end{bmatrix}.$$

Each column represents a partial derivative of AGC model with respect to a parameter. Furthermore, the matrix  $(H^T(\theta)H(\theta))$  in Step 4 can be analytically computed to bypass inner product calculation [1]. This will significantly accelerate the algorithm. Step 5 checks for local stop criteria, if the improvement in the parameter vector is greater than a preset tolerance (*tolerance1*) or the number of iterations exceeds a preset number (*kMax*) the inner-loop terminates and the algorithm proceeds with Step 6. Otherwise the parameter vector is updated and the process starts with the new iteration on Step 3. Step 6 checks for global convergence by comparing the improvement in the parameter vector against another preset tolerance (*tolerance2*). If this is satisfied the algorithm stops, otherwise the parameter vector is updated and algorithm proceeds with Step 2.

Using the parameter estimation algorithm above, the parameters of the AGC model is optimized to represent pulse-echo waveforms obtained from planar surface reflectors. Figure 2 shows four different echo measurements and estimations. Figure 2.a shows a measured echo (blue line) from a planar front surface reflector in water using a 5 MHz broadband transducer. The envelope of this echo (see Figure 2.a) is of skewed shape and tapers off slowly. The AGC represents this envelope with a good accuracy and the sinusoidal chirp tracks the frequency drift noticeable in the echo. Figure 2.b shows another measured echo (dotted line) from a back-surface reflector using the same transducer as in Figure 1.a. Figure 2.c and Figure 2.d show a front-surface echo and a back-surface echo measured using a 10 MHz broadband transducer. The AGC model represents the measured echoes fairly well. For comparison, we tested the Gaussian Chirplet echo model on these echoes. Figure 3 shows the echo estimation results in the same order as in Figure 2. One can visually observe the better fits with the AGC model. The symmetric envelope limitation of the Gaussian Chirplet model is overcome with the AGC model.

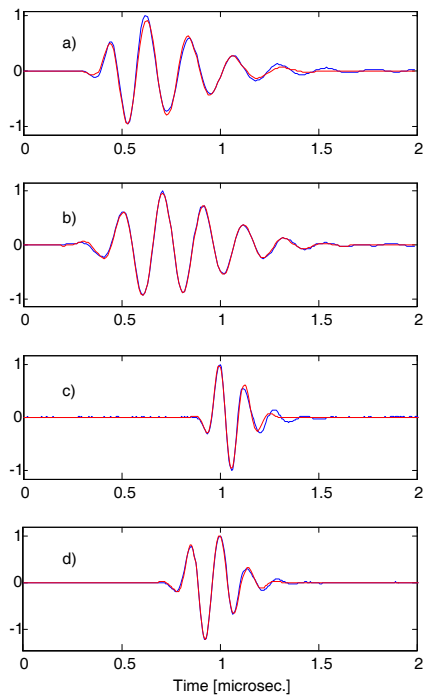


Figure 2. AGC model fitting on several echoes obtained from flat surface reflectors using two different transducers: a) The estimated echo (solid red) for a measured echo (dotted blue) from a flat surface reflector in water (a 5 MHz broadband transducer is used), b) The estimated echo (solid red) for a measured echo (dotted blue) from a back surface reflector in water for the same transducer used in (a), c) The estimated echo (solid red) for a measured echo (dotted blue) from a flat surface reflector in water (a 10 MHz broadband transducer is used), d) The estimated echo (solid red) for a measured echo (dotted blue) from a back surface reflector in water for the same transducer used in (c).

#### IV. SPARSE REPRESENTATION OF ULTRASONIC ECHOES USING AGC MODEL

Sparse signal decomposition methods based on a matching pursuit approach has been extensively used in ultrasonic NDE to represent complex ultrasonic signals in terms of model echoes. Parametric echo models such as Gaussian echo and Gaussian Chirplet have been used to represent ultrasonic echo structures [3, 4, 8]. The new AGC model can be used in place of these models. This model is incorporated in a sparse signal decomposition algorithm presented in [8].

To demonstrate the AGC model in a signal decomposition algorithm, we use ultrasonic data acquired from a steel block that contains a flaw (see Figure 4.a) using a broadband transducer with a center frequency of 5 MHz. The sampling rate is 200 MHz. The decomposition signal is displayed in Figure 4.a in solid red line along with the measured signal in dotted blue line. Furthermore, the TFR of the decomposed Gaussian echoes using the TF estimation technique described in [8] is shown in Figure 4c. The TFR obtained via this type of decomposition can be useful for feature extraction. In particular, flaw detection in large-grained materials is challenging because the grain scattering echoes dominate the flaw echoes. In the Rayleigh scattering region, it has been shown that grain scattering results in an upward shift in the expected frequency of the ultrasonic signal [8]. On the other

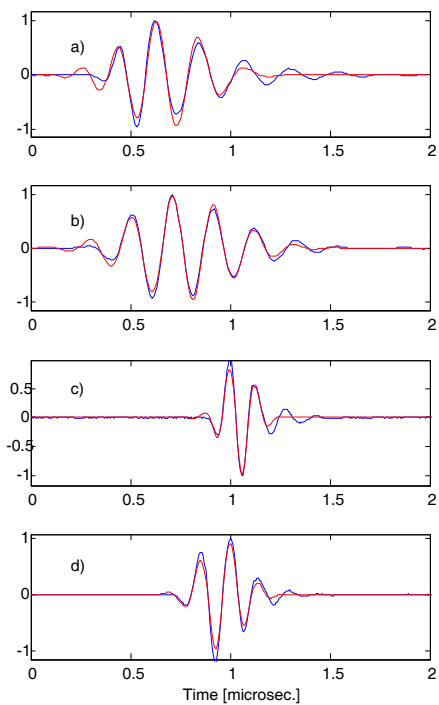


Figure 3. Gaussian Chirplet model fitting on the measured echoes shown in Fig. 2. The model fits can be compared to those of AGC shown in Figure 2.

hand, flaw echoes exhibit a downward shift in their expected frequency due to the overall effect of attenuation because flaws are generally larger in size than the grain hence behave like geometrical reflectors. In summary, the flaw echoes exhibit high energy profiles at low frequency levels while grain echoes exhibit low energy profiles at high frequency levels [8]. This downward frequency shift of the flaw echo can be utilized as a discrimination tool. The high energy density circles at low frequency levels in the TF contour plot (see Figure 4c) represent the flaw echo. One can determine the exact location, frequency and energy of this echo by examining the parameters of the associated AGC function.

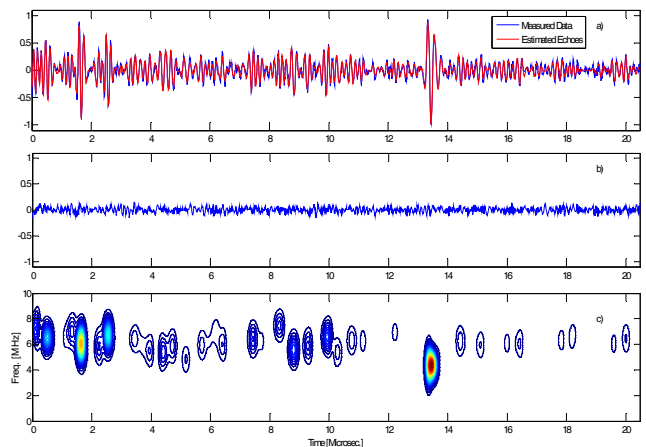


Figure 4. Sparse representation of microstructure grain echoes and a flaw echo using AGC model: a) Measured echo and sparse decomposition using 54 AGC model echoes, b) Residual signal after estimation, c) TF representation after decomposition.

The AGC model is also tested for the analysis of reverberation echoes acquired from a multi-layered test specimen [10]. The test specimen is prepared by placing an aluminum plate and a steel block in water, where there is a gap (water) between the plate and the block. The echoes are captured with a 10 MHz nominal frequency transducer and sampled with 100 MHz frequency. These echoes are shown in Figure 5.a along with the estimated echoes. The arrival times and amplitudes of the estimated echoes are shown in Figure 5.b. The model echoes fit the measured echoes with very reasonable accuracy. The parameters of the model can be further analyzed to estimate test parameters, for example, the thickness of each layer, attenuation coefficient, etc. [10].

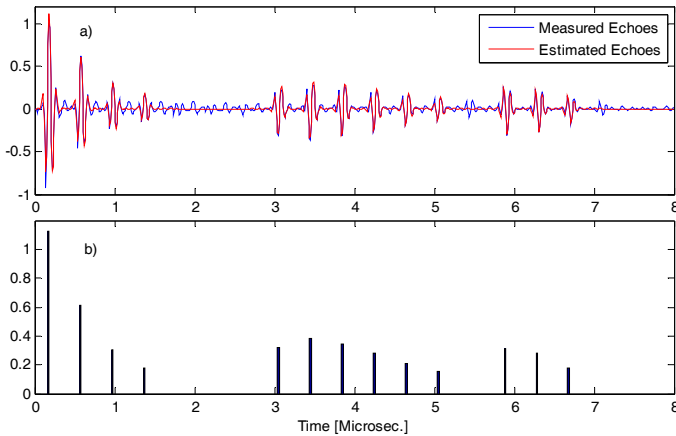


Figure 5. Parameter estimation of reverberation echoes: a) Reverberation echoes measured from a multi-layered material and estimated echoes (blue line) and estimated echoes (red line) using the AGC model, b) Arrival times and amplitudes of the estimated echoes.

## V. CONCLUSIONS

In this study we introduced the AGC echo model with an asymmetric envelope and linear chirp sinusoidal. This model is designed to represent echoes from planar surface reflectors and geometric reflectors when using piezoelectric transducers in pulsed excitation. We developed an optimization algorithm to estimate the parameters of this model. The model is tested using echo measurements from planar surface reflectors obtained from different transducers. It has been shown that the proposed model can represent diverse shape echoes better than the existing echo models. We also incorporated this AGC model in a sparse decomposition algorithm and test it for real ultrasonic measurements such as grain scattering and flaw echoes in a microstructure material, and reverberation echoes from a multi-layered material. In summary, this model

generalizes previously used Gaussian echo and Gaussian Chirplet models, offers a greater flexibility in sparse decomposition, and likely to improve the performance of model-based ultrasonic echo estimation techniques.

## VI. ACKNOWLEDGMENT

This research is partially supported by the NSF grant number IIP-0917690.

## REFERENCES

- [1] R. Demirli and J. Saniie, "Model-based estimation of ultrasonic echoes, part I: analysis and algorithms", *IEEE Trans. on Ultrasonics Ferroelectrics and Frequency Control (UFFC)*, Vol. 48, No. 3, pp. 787-802, May 2001.
- [2] R. Demirli and J. Saniie, "Model-based estimation of ultrasonic echoes, part II: nondestructive evaluation applications", *IEEE Trans. on UFFC*, Vol. 48, No. 3, pp. 803-811, May 2001.
- [3] G. Cardoso and J. Saniie, "Ultrasonic data compression via parameter estimation", *IEEE Trans. on Ultrasonics Ferroelectrics and Frequency Control*, Vol. 52, No. 2, pp. 313-325, February 2005.
- [4] Yufeng Lu, R. Demirli, G. Cardoso and J. Saniie, "A successive parameter estimation algorithm for chirplet signal decomposition", *IEEE Trans. on Ultrasonics Ferroelectrics and Frequency Control*, Vol. 53, No. 11, pp. 2121-2131, November 2006.
- [5] L. Satyanarayan, K. B. Kumaran, C.V. Krishnamurthy and K. Balasubramaniam, "Inverse method for detection and sizing of cracks in thin sections using a hybrid genetic algorithm based signal parametrisation", *Theoretical and Applied Fracture Mechanics*, Vol. 49, Issue 2, pp. 185-198, April 2008.
- [6] Dencks, S.; Barkmann, R.; Padilla, F.; Laugier, P.; Schmitz, G.; Gluer, C, "Model-based estimation of quantitative ultrasound variables at the proximal femur," *IEEE Trans. on Ultrasonics, Ferroelectrics and Frequency Control*, , vol.55, no.6, pp.1304-1315, June 2008.
- [7] Y. Lu and J.E. Michaels, "Numerical implementation of the Matching Pursuit for the analysis of complex ultrasonic signals", *IEEE Trans. on Ultrasonics Ferroelectrics and Frequency Control*, Vol. 55, No. 1, pp. 173-182, January 2008.
- [8] R. Demirli and J. Saniie, "An efficient sparse signal decomposition technique for ultrasonic signal analysis using envelope and instantaneous phase", *Proc. of the IEEE Int. Ultrasonics Symposium*, pp. 1376-1379, October 2008.
- [9] S. Mallat and Z. Zhang, "Matching pursuits with time-frequency dictionaries", *IEEE Trans. on Signal Processing*, Vol. 41, pp. 3397-3415, December 1993.
- [10] Y. Lu, R. Demirli, E. Oruklu, and J. Saniie, "Estimation and Classification of Ultrasonic Echoes backscattered from multilayered materials", *Proc. of the International Congress on Ultrasonics*, pp. 1590-1593, April 2007.
- [11] S.M. Kay, *Fundamentals of Statistical Signal Processing* (Prentice Hall, New Jersey, 1993).